AUTOMATIC MESH GENERATION FOR FINITE ELEMENT CALCULATIONS IN THE CASE OF THERMAL LOADS

H. CORDS and R. ZIMMERMANN

Institut für Reaktorwerkstoffe,
Kernforschungsanlage Jülich GmbH, D-517 Jülich, Germany

SUMMARY

The presentation describes a method to generate finite element nodal point networks on the basis of isothermals and flux lines. Such a mesh provides a relatively fine partitioning at regions where pronounced temperature variations exist. In case of entirely thermal loads a net of this kind is advantageous since the refinement is provided at exactly those locations where high stress levels are expected.

In the present contribution the method was employed to analyze the structural behaviour of a nuclear fuel element under operating conditions. The graphite block fuel elements for high temperature reactors are of prismatic shape with a large number of parallel bores in the axial direction. Some of these bores are open at both ends and cooling is effected by helium flowing through. Blind holes contain the fuel as compacts or cartridges.

The basic temperature distribution in a horizontal section of the block was obtained by the boundary point least squares method which yields analytical expressions for both temperature and thermal flux. The corresponding computer code was presented at an earlier SMiRT conference.

The mesh generation programme requires values of temperature T and flux ϕ on the boundary of the region to be partitioned. In a diagramme with coordinate axes T and ϕ these boundary values form a closed contour. The complex function $w=T(x, y)+i\phi(x, y)$ maps the original geometry onto the (T, ϕ)-plane in which isothermals and flux lines are two sets of parallel lines orthogonal to each other. The points of intersection including those on the boundary are used to generate a mesh in a conventional manner. The network is composed of triangular elements with three nodal points each with specified topology.

Finally the mesh in the (T, ϕ)-plane is mapped back onto the original geometry given in $z=x+iy$ coordinates by employing techniques of the theory of functions.

$$z(w_0) = \frac{1}{2\pi i}\oint^{B} \zeta \frac{w'(\zeta)}{\dot{w}(\zeta)-w_0}\,\mathrm{d}\zeta$$

The method is particularly useful for regular arrays of heat sources and sinks as encountered in heat exchanger problems. The generated mesh matches the requirements of a subsequent structural analysis with finite elements provided there are no other than thermal loads.

1. Introduction

Calculations employing the finite element method without exception require a detailed, geometrical description of the structure. Usually the specimen under investigation is subdivided into several hundred, basic, structural elements interconnected by nodal points. The network has to be specified in terms of nodal point coordinates, nodal point numbers and element numbers. In order to minimize the labour involved and the subsequent search for errors, a number of authors recently suggested computer algorithms for mesh generation with varying degree of automation [1-3].

The present approach to a mesh generating algorithm is applicable in the case of exclusively thermal loads and, furthermore, requires a preceding, steady state, thermal calculation according to the "boundary point least squares method" [4]. These rather special conditions are encountered in the thermal and stress analysis of prismatic nuclear fuel elements as used for High Temperature Gas-cooled Reactors. Block-type fuel elements are of prismatic, hexagonal shape with a large number of axial channels for both fuel sticks and the flow of coolant. Usually each coolant channel is surrounded by six fuel channels, such that the transport of heat proceeds predominantly in a horizontal direction. Assuming constant flux of neutrons throughout the horizontal section and axisymmetric nuclear loading and cooling, the two-dimensional problem can be reduced to that pertaining to a symmetry section of the horizontal cross section. The symmetry element of a nuclear fuel element shown in Fig. 1 contains a regular hole pattern and is bounded by adiabatic lines. Thermal analyses of heat exchangers can be considered as related problems.

The finite element method demands mesh refinements where a strong variation of the solution is expected, particularly in the case of constant strain elements. Since the variation of temperature causes differential, thermal expansion and therefore stresses, the suggestion to use equipotentials of temperature and heat flux as a basis for the finite element mesh is natural. Moreover, isothermals and flux lines being two orthogonal sets of lines would produce nearly rectangular, quadrilateral elements which may easily be subdivided to yield nearly rectangular triangles. However the special requirements introduced by stress concentrations cannot be met by the isothermal mesh. With respect to the application to nuclear fuel elements it should be pointed out that only initially are the mechanical loads entirely thermal. Nevertheless, under irradiation by fast neutrons, the differential shrinkage closely follows the original temperature distribution.

2. Thermal Analysis

The boundary point least squares method may be regarded as a limiting case of the finite element method. The geometry is partitioned into a few or only one element. On the other hand the trial functions are of extremely complex structure, and a large number of boundary conditions are required to determine the unknown coefficients. The boundary points are generated

automatically along straight lines and circular arcs. Several boundary conditions may be specified [4].

The trial functions are chosen such that the heat conduction equation is satisfied. In principle any of the functions treated in the analytic function theory is suitable. Polynomials in the complex variable z have the additional advantage that all unknown coefficients are involved linearly. In conjunction with linear boundary conditions the evaluation of the coefficients leads to a linear system of simultaneous equations which is easily solved.

Usually a power series is expanded about the centre z_0 of each of the holes (Fig. 1) representing either a heat source or a sink.

$$w_1(z) = c \cdot \ln(z - z_0) + \sum_{n=0}^{S} a_n (z - z_0)^n \qquad (1)$$

The real and imaginary parts of the complex function w(z) represent temperature T and thermal flux ϕ, respectively. In order to match the adiabatic boundary conditions imposed by the two symmetry lines of the symmetry section (Fig. 1) a trial function has to be constructed in which the imaginary part either vanishes or is a constant along the symmetry lines. The required symmetry in the trial function is achieved by superposing power series of the type (1) with expansion centres z_ν and $\bar{z}_\nu$ symmetrically positioned with respect to both symmetry lines. The complete set of expansion centres is shown in Fig. 3.

$$z_\nu = z_0 \, e^{-2\nu i \pi/m} \qquad \nu = 0, 1, 2, \ldots\ldots m-1 \qquad (2)$$

The integer m is determined by the centre angle of the symmetry section. The fully symmetric series expansion for one hole is given by

$$w_2(z) = \sum_{\nu=0}^{m-1} \{c \ln(f_\nu(z)) + \bar{c} \ln(f_{\nu+1}(z))\} + \sum_{n=0}^{S} \sum_{\nu=0}^{m-1} \{a_n (f_\nu(z))^n + \bar{a}_n (f_{\nu+1}(z))^n \qquad (3)$$

with $\quad f_\nu(z) = (z - z_\nu) \cdot \bar{z}_\nu / |z_\nu|$

and $\quad f_{\nu+1}(z) = (z - \bar{z}_{\nu+1}) \, z_{\nu+1} / |z_{\nu+1}|$

All of the remaining sources and sinks yield similar contributions to the trial function w of the symmetry element.

$$w = \sum w_2(z) \qquad (4)$$

Special trial functions containing source terms had to be devised for fuelled regions. The computer code described in ref. [4] was altered to yield additionally the imaginary part of w. The data output now comprises three sets of complex numbers

$$z_j, \; w(z_j) \text{ and derivative } w'(z_j) \qquad (5)$$

where z_j uniformly covers the boundary line of the domain to be meshed.

3. Mesh Generation

The symmetry element shown in Fig. 1 may serve as an example to describe the algorithm. The hatched areas are source regions and are excluded from the procedure. The domain to be meshed must be divided into three subregions corresponding to the heat-catchment areas of the three cooling channels. This provision is necessary to ensure that w(z) is a single-valued, analytic function with respect to each subregion. By use of the function w(z) all of the subregions are mapped onto a plane with coordinate axes T and Ø, which designate temperature and thermal flux, respectively (Fig. 2).

Subsequently all subregions are treated the same. The mapped domain of subregion 3 is also shown in Fig. 4. In the w-plane, isothermals and flux lines are two orthogonal sets of straight lines. These are specified to the code by stating an initial value w_o, width $\Delta w=(\Delta T, \Delta \emptyset)$ and the number of lines for both directions such that subregion 3 is completely covered. Points of intersection w_{ij} that fall beyond the bounds C of the domain D are rejected by means of the criterion

$$\frac{1}{2\pi i} \oint_{C} \frac{dw}{w-w_{ij}} = \begin{cases} 0 & \text{for } w_{ij} \notin D \\ 1 & \text{for } w_{ij} \in D \end{cases} \qquad (6)$$

Having established the internal nodal points w_{ij} the next step of the employed strategy is to determine the points of intersection of both the isothermals and the flux lines with the boundary C. This set of points, w_k, and the corresponding originals, z_k, are obtained by interpolation of $w(z_j)$ and z_j (see (5)), respectively. Corner points of the original boundary curve $B = w^{-1}(C)$ (see + in Fig.4) are included in w_k by definition. Points w_k too closely spaced and internal points w_{ij} too close to the boundary are dicarded.

The nodal point numbering starts with all nodal points on the boundary, which generally causes an awkwardly conditioned stiffness matrix [5]. For this reason it was found that a subsequent renumbering of the finalised mesh was necessary to obtain a smaller band-width. In a first loop around the boundary C, (see arrow in Fig. 4), for any two consecutive boundary points w_k, an internal nodal point w_{ij} or a third boundary point w_k is selected to form a triangular element. Where there is a choice of several points, it is made on the basis of the largest angle subtended by the boundary segment. In the first loop, all element sides which do not have contiguous elements are registered as open sides. The following loops complete triangles from the set of open sides generated in the previous loop. In all cases the criterion of largest, opposite angle is utilised. In this way the triangulization proceeds like a helix from the boundary towards the centre of the domain.

The finalised mesh including the element specification is then conformally mapped back onto the z-plane. With respect to the boundary, the mapping is performed by interpolation of the original boundary curve B, specified by (5). The internal, nodal points are transferred employing the

residue theorem known in the theory of functions [6].

$$z_{ij}(w_{ij}) = \frac{1}{2\pi i} \oint_B z \, \frac{w'(z)}{w(z) - w_{ij}} \, dz \tag{7}$$

The line integral is evaluated numerically according to Simpson's rule for definite integrals and employing the point sets (5). A consistency check on the analytic properties of $w(z_j)$ and $w'(z_j)$ as well as on the quality of the integration method can be performed by means of the integral

$$1 = \frac{1}{2\pi i} \oint_B \frac{w'(z)}{w(z) - w_{ij}} \, dz \tag{8}$$

which should yield exactly 1 for all internal points w_{ij}. Finally the networks for the subregions are interconnected to give a mesh for the whole symmetry section.

The renumbering algorithm is based on the following strategy. The nodal point numbers are fitted by means of a linear, least squares fit to the quadratic form

$$n(x,y) = \sum_{ij=0}^{2} a_{ij} \, x^i \, y^j \tag{9}$$

where x and y are the coordinates of the z-plane. Any two nodal point numbers strongly deviating from the surface in different directions are interchanged if, additionally, the mean square deviation becomes smaller by that operation.

4. Results and Conclusion

The complete mesh generated for the three simply connected subregions is shown in Fig. 5 a. The network is composed of 755 elements and 464 nodal points. It consists of a regular interior part, with rectangular triangles, and an irregular part which is the connection with the boundary. Fig. 5 b displays the mapped mesh covering the symmetry section given in the (x,y)-plane. The regular part is composed of nearly rectangular triangles. The transition between sizes of neighbouring elements is gradual. The connection with the boundary and those between subregions are somewhat less satisfactory. The more acute angles occurring on the outer regions of the symmetry section are related to the small density of flux lines. These areas of the nuclear fuel block do not take part in the interchange of heat. The situation can be somewhat improved by requesting a finer grid of flux lines.

Fig. 6 shows the temperature distribution in the form of a three-dimensional projection. The finite element mesh is so used that each nodal point is raised by the amount of the corresponding temperature value. Therefore isothermals appear to be running in horizontal planes. The mesh has been refined manually at the two locations where stress concentrations were expected to occur. These locations are marked on Fig.7 which shows the corresponding stress distribution. It is apparent from Fig. 7, that apart

from the stress concentrations the larger stresses occur on the surface of the coolant channels and on the surface of fuel channels opposite coolant holes. This is exactly in those regions where the mesh generation algorithm provides refinement (Fig. 5 b).

The symmetric matrices shown in Fig.8 reflect the nodal point numbering system. The diagonal represents the successive numbering from 1 to 464 nodal points gathering each 4 numbers into one star. Numbers of neighbouring nodal points are recorded in the same row or column and the corresponding stars appear at a distance proportional to the difference in numbering. The three fork-like structures of the matrix in Fig. 8a correspond to the three sub-regions. The reduced band-width shown in Fig. 8b was achieved by 3500 inter-changes of nodal point numbers. However, during the last 2000 interchanges the bandwidth did not improve considerably.

The problem of providing a triangular mesh with smoothly varying mesh spacing has been solved satisfactorily by employing equipotential line sets. The applicability of the method has been tested in stress analyses of nuclear fuel elements. It is expected that a similar approach will be useful in diffusion, electrostatic and electromagnetic problems where the governing, differential equation is also the Laplace equation.

References

[1] FUKUDA, J., SUHARA, J., "Automatic mesh generation for finite element analysis", Advances in Computational Methods in Structural Mechanics and Design, UAH Press, Huntsville, Alabama, 1972

[2] FREDERICK, C.O., WONG, Y.C., EDGE, F.W., "Two-dimensional automatic mesh generation for structural analysis", Int. J. num. Meth. Engng, 2, 133-144 (1970)

[3] ZIENKIEWICZ, O.C., PHILLIPS, D.V., "An automatic mesh generation scheme for plane and curved surfaces by isoparametric coordinates" Int. J. num. Meth. Engng, 3, 519-528 (1971)

[4] HULBERT, L.E., "Heat conduction in multiconnected composite regions with radiation boundary conditions", SMiRT 1971, L 2/2

[5] LORENZ, K.W., "Finite Elemente in der Statik", Editor: K.E. Buck, Verlag Wilhelm Ernst und Sohn, Berlin 1973, p. 373

[6] KNOPP, K., "Funktionentheorie I, Grundlagen der allgemeinen Theorie der analytischen Funktionen", Sammlung Göschen Band 668, Walter de Gruyter Co, Berlin 1957, p. 130-138

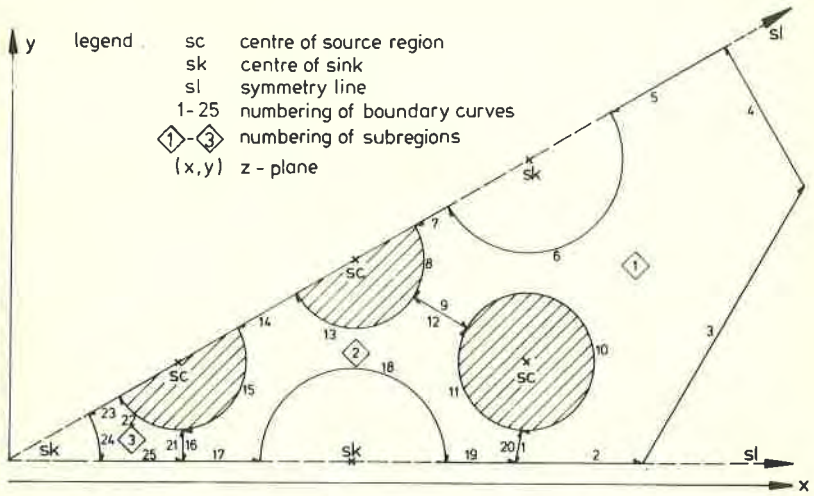

Fig. 1. Symmetry element of horizontal cross section of nuclear fuel element

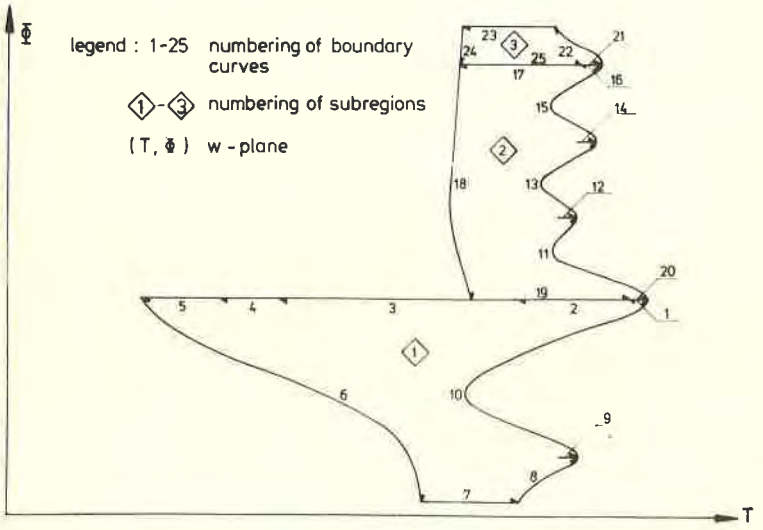

Fig. 2. Symmetry element of fig. 1 mapped onto the (T, Φ) - plane

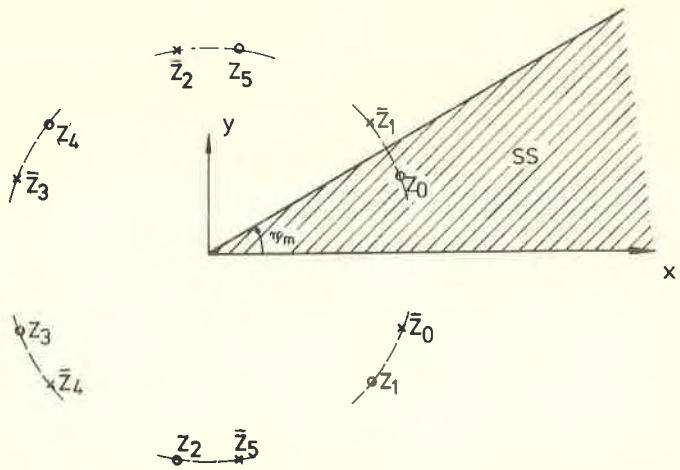

Fig.3. Complete set of symmetry poles Z for a symmetry section SS

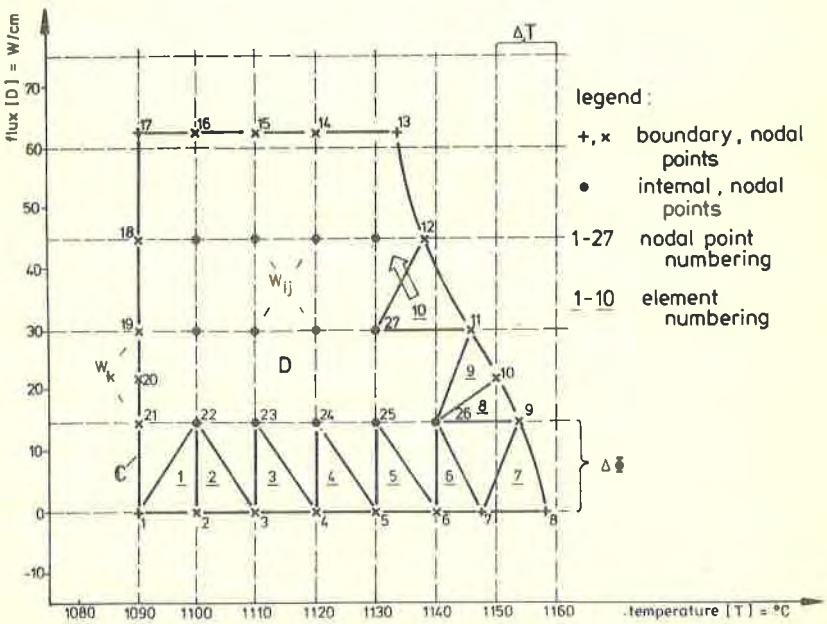

Fig.4. Mesh generation of the mapped subregion 3

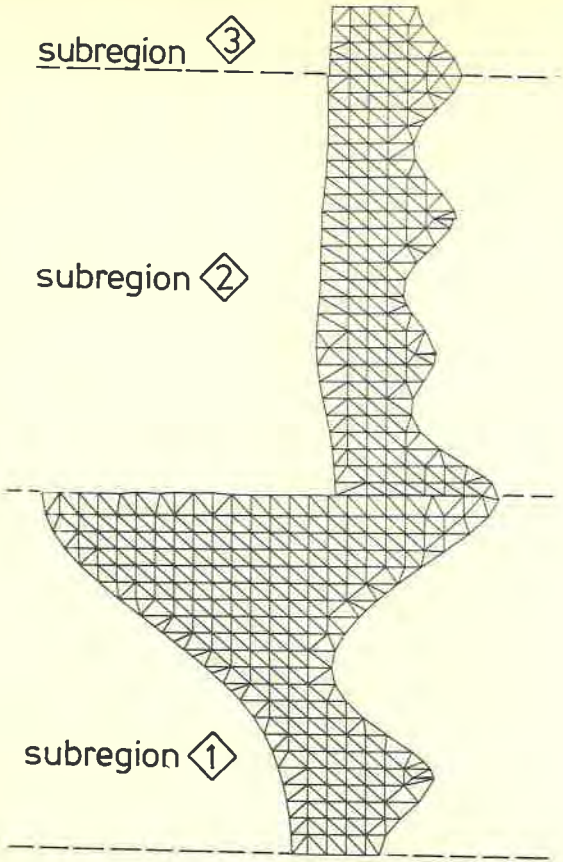

a) w - plane

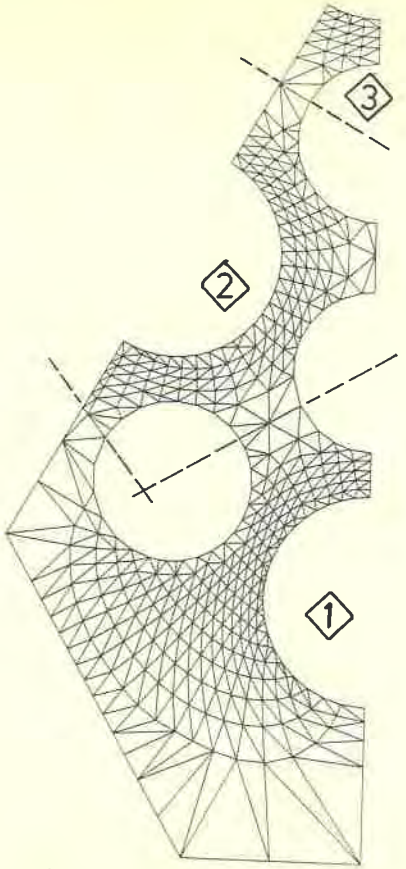

b) z - plane

Fig. 5. Finalised mesh for both planes

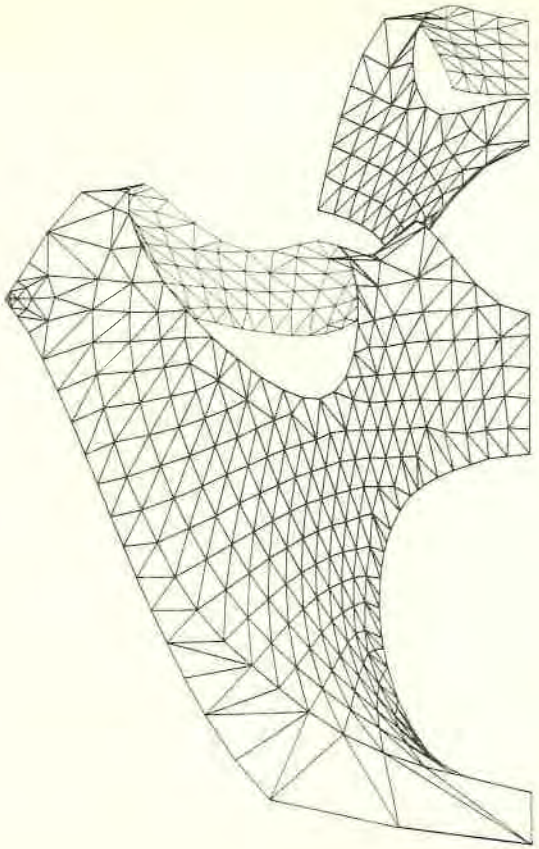

Fig. 6 3-dimensional representation of the temperature distribution utilising the generated nodal point mesh

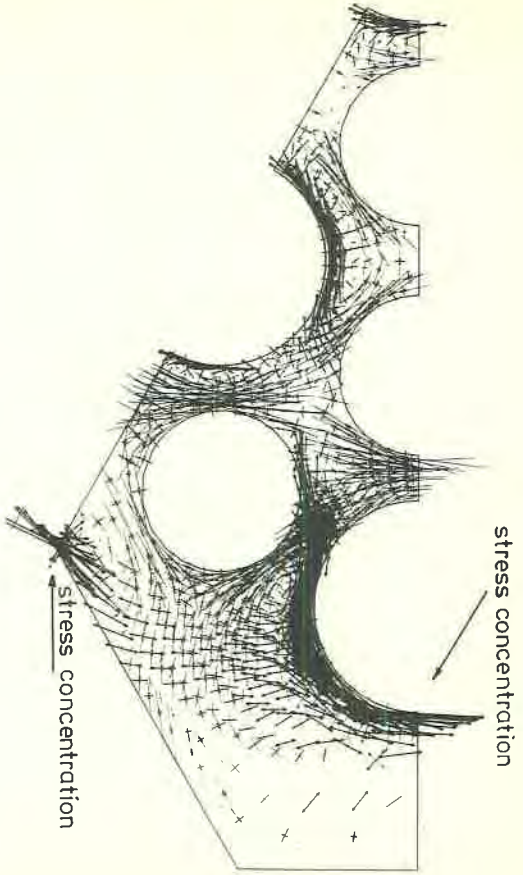

Fig. 7 Vector diagram of principal stresses calculated on the basis of the temperature distribution shown in fig. 6

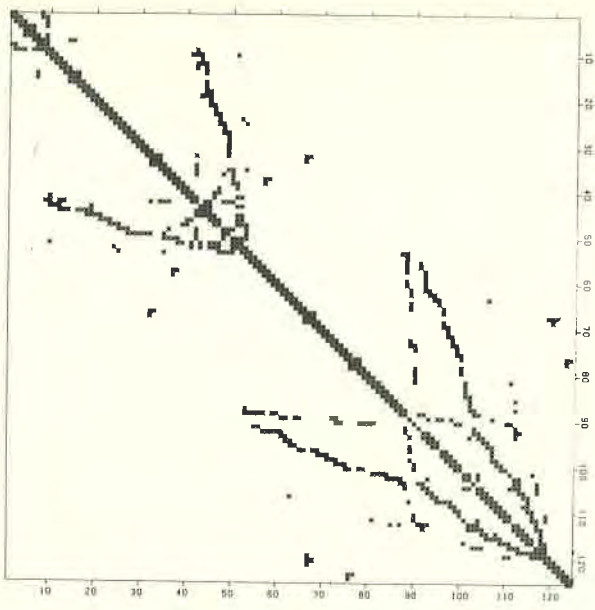

a) as produced by the mesh generating algorithm

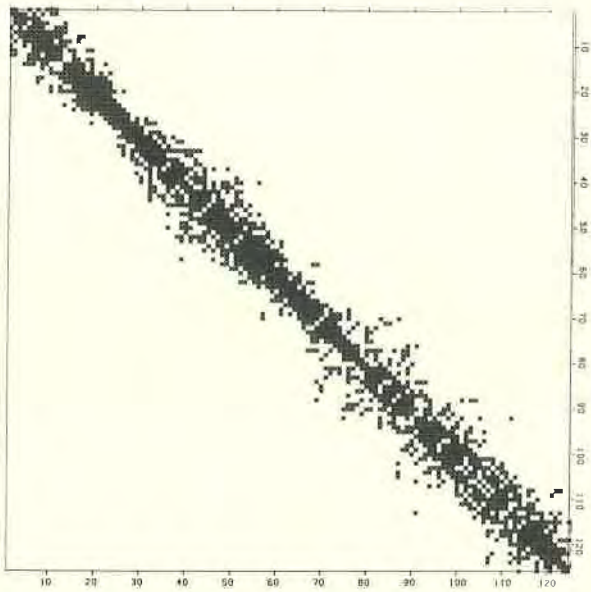

b) after band-width minimisation

Fig. 8. Matrix of neightbouring nodal points